Switching protein metalloporphyrin binding specificity by design from iron to fluorogenic zinc

Benjamin J. Bowen[a,†], Adam R. McGarrity[a,†], Jenn-Yeu A. Szeto[a], Christopher R. Pudney[b], D. Dafydd Jones[a*]

Metalloporphyrins play important roles in areas ranging from biology to nanoscience. Using computational design, we converted metalloporphyrin specificity of cytochrome b_{562} from iron to fluorogenic zinc. The new variant had a near total preference for zinc representing a switch in specificity, which greatly enhanced the negligible aqueous fluorescence of free ZnPP *in vitro* and *in vivo*.

Here, we describe how computational design can change the metalloporphyrin specificity of cytochrome b_{562} (cyt b_{562}), a b-type haem binding protein unit, from iron to fluorogenic and photochemically active zinc. Metalloporphyrins [1] represent an important class of organometallic compounds and play a major role in biology as essential cofactors to enable protein function in processes ranging from light harvesting to electron transfer to enzyme catalysis to O_2 transport [2]. Binding to a protein tunes and modulates the metalloporphyrin physiochemical properties. The metal centres used in biology are Fe (e.g. haem), Mg (e.g. chlorophyll) and, to a much lesser extent Co (Vitamin B12) and Ni (F430). This does not however represent the full metal repertoire available to porphyrins (e.g. Cu, Pt, Ag, Cd, Ir, Zn) [1]. There is currently great interest in incorporating new metal cofactors into proteins. Such abiotic cofactors have recently been shown to confer new enzymatic catalytic routes [3, 4]. Zinc porphyrins such as zinc protoporphyrin IX (ZnPP, Figure 1a) are one such class, playing important roles in clinical (including cancer therapy) and nanoscience settings. While ZnPP is not naturally utilised in biology as a protein cofactor, its aberrant presence in blood is commonly used to diagnose haem metabolism disorders [5]. The photo-induced electron and energy transfer properties of zinc porphyrins make them particularly attractive for nanoscale applications, ranging from photosensitizers in solar cells to molecular optoelectronic components [6-9]. ZnPP is inherently fluorescent but substantially quenched in aqueous solution [10, 11]. Designer protein components have the potential to further enhance ZnPP use through: (i) activation of fluorogenic properties [12] in aqueous conditions as an aid to clinical sensing and cell imaging; (ii) providing an organised, defined and tunable self-assembling scaffold for nanodevice construction [6, 13-17].

ZnPP incorporation within a protein scaffold has classically been achieved by either: (i) metal centre exchange (in the case of covalently attached porphyrins) that require harsh conditions unsuitable for most biological settings [13, 18, 19]; (ii) facile exchange in the case of non-covalent porphyrin-protein complexes [11, 20]. With regards to the latter, affinity for ZnPP is inherently low, with preference for the original haem cofactor; little attention is paid to optimising the protein interaction despite the structural and physicochemical variations on exchanging the porphyrin metal centre (Fig 1a). Here we show how computational design has been used to switch cyt b_{562} specificity from its normal iron porphyrin (haem) to zinc. The new protein can activate ZnPP fluorescence both *in vitro* and *in vivo*.

Figure 1. Porphyrin structure and cyt b_{562} variants. (a) Structure of haem (cyan) and ZnPP (green). The metalloporphyrin structure geometries were optimised using GAMESS-US [21]. (b) Sequences of the cyt b_{562} variants and their corresponding nomenclature. The methionine that coordinates Fe in haem is highlighted with *. (c) Model of ZnPP-bound cyt b_{562}^{ZnPP} with the residues mutated that shift metalloporphyrin specificity highlighted.

Cyt b_{562} (Figure S1) is a small, helical bundle protein that binds haem non-covalently [22-24]. It is an important model for electron transfer [25-28], engineering novel components [29-34] and assembling supramolecular structures [6, 14, 35]. ZnPP can replace haem through passive exchange [20, 33, 36] but the environment is non-ideal resulting in relatively low affinity binding (404 nM ±11

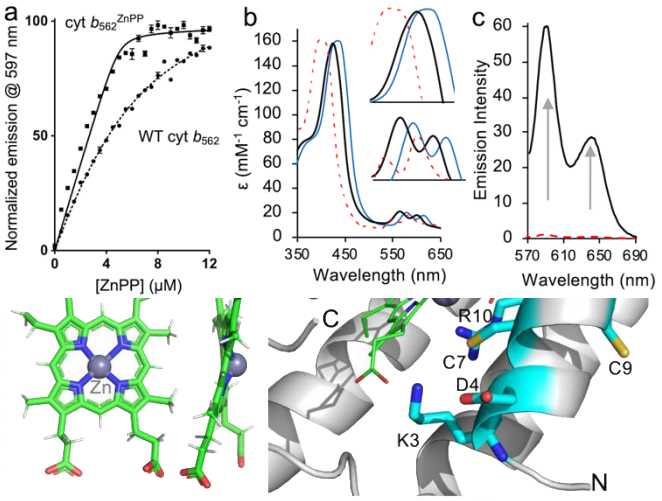

K_D; Table S1) and a significant background haem binding *in vivo* (*vide infra*). Factors include non-optimal metal coordination ligands and change in tetrapyrole structure and planarity due to the larger ionic radius of Zn^{2+}(Fig 1a) [37, 38].

Figure 2. Absorbance and fluorescence properties of cyt b_{562}^{ZnPP} binding variants. (a) ZnPP titration into 5 μM cyt b_{562}^{ZnPP} (full line) or WT cyt b_{562} (dashed line). (b) absorbance spectra of free ZnPP (dashed red line), wt cyt b_{562} (blue line), and cyt b_{562}^{ZnPP} (black line). Inset is the Soret peak (top) and α/β bands (bottom). (c) fluorescence emission spectra (on excitation at 431 nm) of ZnPP in the presence (black line) and absence (red dashed line) of cyt b_{562}^{ZnPP}.

The first stage in the design process was to optimise Zn coordination. Zn coordination is normally through soft ligands such as the cysteine thiol group and the imidazole group of histidine, or base ligands from the carboxylate groups of aspartate and glutamate; the native M7 *S*-methyl thioether group is not ideal. This was confirmed through computational analysis with cysteine considered the best, albeit still relatively poor, alternative (the M7C mutation; Figure S2). The second

native axial ligand, the imidazole group of H102, was considered optimal so was not changed (Figure S2). The M7C variant was generated and the measured ZnPP and haem affinity (dissociation constant, K_D) were comparable (181 ±11 nM for ZnPP and 206 ±2 nM for haem; Table S1) so generating a starting mutant with slightly improved ZnPP binding and lower haem affinity. Replacement of Met7 with either His (a second potential coordinating ligand) or Gly lowered ZnPP binding affinity to that of wild-type cyt b_{562} with the *bis*-His mutant retaining specificity for haem (Table S2). The absorbance spectrum of cyt b_{562}^{M7C} (Fig S3) confirms ZnPP binding to the protein as indicated by the red shift in the Soret peak at 418nm for free ZnPP to a sharper peak at 431nm. The Soret and α/β band peaks of cyt b_{562}^{M7C} are slightly blue shifted (8-10 nm) compared to the ZnPP bound to wild-type cyt b_{562}. The Soret peak is also broader for wt cyt b_{562} suggesting a mixed binding population compared to cyt b_{562}^{M7C}. The ZnPP α/β peaks ratio also switches on cyt b_{562} binding.

To further optimise ZnPP binding, a more systematic *in silico* mutagenesis approach was adopted. Using the wt holo cyt b_{562} crystal structure [39] as a starting point, every residue from 1 to 20 was replaced to every possible residue and energy minimised to avoid clashes. The structures derived from the energy minimisation were used as the starting point for docking simulations using AutoDock [40] and Rosetta LigandDock [41]. As a test for the accuracy, the *in silico* derived binding energy of wt cyt b_{562} was compared with the measured K_D. The measured binding energy for wt cyt b_{562} (where $\Delta G = RT \ln K_D$) is -8.7 kcal mol^{-1} for ZnPP, and -11.0 kcal mol^{-1} and for haem. These are close to the binding energies predicted from our modelling approach (Table S1). The *in silico* design process identified a variant with improved ZnPP binding energies termed cyt b_{562}^{ZnPP}. In addition to the M7C mutation, four other mutations were identified (L3K, E4D, T9C, L10R). The affinity of the variant for ZnPP was much lower (34 ±10 nM as an upper estimate based on fluorescence) compared to wt cyt b_{562} (Figure 2a; Table S1 and Figure S4) with minimal haem binding observed both *in vivo* (Figure 3a) and *in vitro* (Figure S4a). This represents a near total switch in specificity from haem to ZnPP. Mutation R10 arose in the later stages of the design and is buried in the holo form of the protein (Fig 1c) so it was surprising that not only was the L10R mutation tolerated but improved binding. Mutating residue 10 to either alanine or serine reduced affinity for ZnPP to >100 nM (Table S2). Analysis of the model suggests that the guanidinium group of R10 lies within 2-3 Å of the C7 thiol group (Fig 1c and S5a); proton abstraction by R10 may generate a thiolate group, which is a better ligand for Zn binding than the C7 thiol. Lys3 may make an ionic bond to one of the carboxyl groups of ZnPP so stabilizing the complex (Supporting Figure S5b). The T9C mutation is difficult to rationalize but mutation to either alanine or serine reduced ZnPP affinity to ~190 nM. The role of the E4D mutation is also unclear but it's shortened side chain length may prevent steric and/or ionic clashes with puckered ZnPP while maintaining a negative charge at residue 4. Cyt b_{562}^{ZnPP} was analysed in more detail.

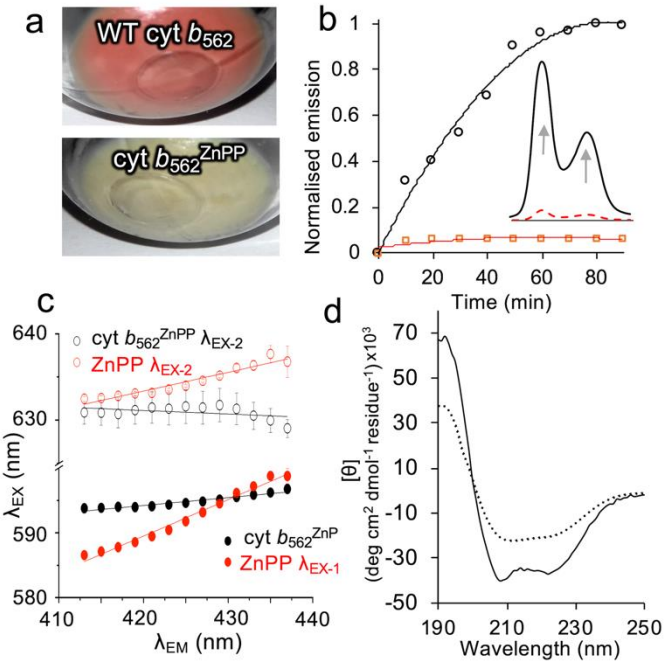

Figure 3. ZnPP binding to cyt b562ZnPP. (a) Cell pellets of recombinantly expressed cyt b562ZnPP and the wild-type protein. (b) Rate of fluorescence emission increase (excitation 431 nm) of E. coli cell culture incubated with ZnPP with cells containing (black line) or without (red line) plasmid-based cyt b562ZnPP. Inset is the fluorescence emission spectra after 1 hr. (c) REES profile (emission wavelength, λEX, versus excitation wavelength, λEM) of free ZnPP (red line) and ZnPP-bound cyt b562ZnPP (black line). EX-1 and EX-2 refer to the two separate emission peaks. (d) CD spectra of apo-cyt b562ZnPP (black dotted line) and cyt b562ZnPP bound to ZnPP (black line).

Cyt b_{562}^{ZnPP} had a characteristic absorbance spectrum indicative of formation of ZnPP holo protein (Fig 2b), with an extinction coefficient of 158 mM cm^{-1} at 424 nm, 5 nm blue shifted compared to wt cyt b_{562}. On binding cyt b_{562}^{ZnPP}, ZnPP fluorescence intensity increased >60 fold (Fig 2b). Excitation at 431 nm gave the expected dual peak emission characteristic of ZnPP [19] (λ_{EM} 590 and 640 nm) with a Stoke's shift of 160 nm and 210 nm (Fig 2b). The peak ratio of the two emission peaks was *circa* 2:1 (590:640 nm). Protein-bound ZnPP could be excited at 431 nm, 550nm and 590 nm (Fig S6). While the brightest emission originated from excitation at 431 nm the ability to excite at multiple and longer wavelengths has obvious benefits for biological imaging. These fluorescence characteristics were observed for wt cyt b_{562} and cyt b_{562}^{M7C} (Fig S7) suggesting that the mutations affected only binding affinity. The quantum yield for the combined emission peaks was measured to be ~92% generating a protein with a brightness of 146 mM^{-1}cm^{-1}, higher than many autofluorescent proteins [42-44]. ZnPP fluorescence is quenched in aqueous solutions to the extent that the quantum yield could not be accurately measured.

Coupled with the fluorogenic properties of ZnPP, cyt b_{562}^{ZnPP} could make a useful genetically encoded imaging agent. A prerequisite for cell imaging is that ZnPP should pass through membranes and have no significant fluorescence in the cell until it binds specifically to cyt b_{562}^{ZnPP}. *E. coli* cells expressing cyt b_{562}^{ZnPP} were colourless in comparison to those expressing wt cyt b_{562} (Figure 3a), which are a pink-red hue due to binding available haem with high affinity [31]. This confirms the near-absent affinity of cyt b_{562}^{ZnPP} for haem. On addition of ZnPP to *E. coli* cells expressing cyt b_{562}^{ZnPP}, fluorescence increased over

time until plateauing after ~40-50 min (Fig 3b). Cells with no plasmid-encoded cyt b_{562} exhibited low baseline fluorescence on addition of ZnPP, which remained steady over the course of the incubation.

Red edge excitation shift (REES) analysis was performed to ascertain the effect of ZnPP binding to cyt b_{562}^{ZnPP} (Fig 3c). REES is an optical phenomenon where decreasing the excitation energy (increasing the excitation wavelength, λ_{EX}) gives rise to a red shift in the maximum of the fluorescence emission (λ_{EM}). Such shifts can arise where the fluorophore exists in a range of discrete solvation environments that are sampled as part of an equilibrium of solvent-solute interaction energies [45]. In some cases, decreasing the energy of excitation allows for photo-selection of the discrete states that are red shifted (lower energy). We have recently demonstrated that for a single fluorophore (tryptophan) containing protein, the REES effect can inform on the equilibrium of conformational states accessible to the fluorophore [46]. The REES data for free and protein-bound ZnPP are shown in Figure 3c and have been extracted for the α/β emission maximum shown in Figure 2b, λ_{EM-1} and λ_{EM-2}, respectively. Free ZnPP exhibits a significant REES effect that is reduced on binding to cyt b_{562}^{ZnPP}; the change in λ_{EM-1} and λ_{EM-2} respectively being 0.56 ± 0.02 nm^{-1} and 0.21 ± 0.02 nm^{-1} for free ZnPP, which reduces to 0.12 ± 0.01 nm^{-1} and -0.04 ± 0.03 nm^{-1} on binding cyt b_{562}^{ZnPP}. These data therefore suggest that the free ZnPP exists in an equilibrium of discrete solvation states and that this equilibrium collapses to essentially a single state on binding to the protein. These data therefore suggest tight ZnPP binding within the core of the protein, with limited solvent access, akin to haem binding. To further confirm ZnPP binding to cyt b_{562}^{ZnPP}, CD spectroscopy was used to monitor the expected transition from a partially folded helical structure to a folded 4-helix bundle on co-factor binding. On addition of ZnPP to cyt b_{562}^{ZnPP}, the deepening of troughs at ~208 nm and 222 nm was observed confirming the increase in helical character, with the spectra of holo-cyt b_{562}^{ZnPP} similar to that observed for wt holo-cyt b_{562} (Fig 3d).

Using systematic computationally guided engineering, the metalloporphyrin specificity of cyt b_{562} can be switched to ZnPP; the affinity is on a par with the natural haem cofactor and represented a near total switch in specificity. More generally, it provides a route for improving affinity of various different haemoproteins for ZnPP and other metalloporphyrins, in which the haem can be replaced by the photosensitizer effect of ZnPP [13, 47] or the catalytic properties of Ir and Cu porphyrins [3, 4]. The design process has shown changing metal coordinating ligands is not the defining step but that optimising residues adjacent to the metal coordination site is critical.

Conflicts of interest

There are no conflicts to declare

Acknowledgements

DDJ would like to thank the BBSRC (BB/H003746/1 and BB/M000249/1), EPSRC (EP/J015318/1) for supporting this work. ARM was supported by a Cardiff School of Biosciences personal studentship. BJB was supported by a SWBio BBSRC DTP studentship. DDJ and ARM would like to thank the Advanced Research Computing @ Cardiff facility, especially Thomas Green for help with access and usage of the Raven cluster.

References

1. K. Kadish, K. M. Smith and R. Guilard, *The porphyrin handbook*, Academic Press, New York, 1999.
2. A. Messerschmidt, *Handbook of metalloproteins*, Wiley, Chichester, 2001.
3. P. Dydio, H. M. Key, A. Nazarenko, J. Y. E. Rha, V. Seyedkazemi, D. S. Clark and J. F. Hartwig, *Science*, 2016, **354**, 102.
4. H. M. Key, P. Dydio, D. S. Clark and J. F. Hartwig, *Nature*, 2016, **534**, 534-537.
5. R. F. Labbe, H. J. Vreman and D. K. Stevenson, *Clin Chem*, 1999, **45**, 2060-2072.
6. J. D. Brodin, J. R. Carr, P. A. Sontz and F. A. Tezcan, *Proceedings of the National Academy of Sciences of the United States of America*, 2014, **111**, 2897-2902.
7. L. L. Li and E. W. Diau, *Chem Soc Rev*, 2013, **42**, 291-304.
8. S. Mathew, A. Yella, P. Gao, R. Humphry-Baker, B. F. Curchod, N. Ashari-Astani, I. Tavernelli, U. Rothlisberger, M. K. Nazeeruddin and M. Gratzel, *Nature chemistry*, 2014, **6**, 242-247.
9. G. Sedghi, V. M. Garcia-Suarez, L. J. Esdaile, H. L. Anderson, C. J. Lambert, S. Martin, D. Bethell, S. J. Higgins, M. Elliott, N. Bennett, J. E. Macdonald and R. J. Nichols, *Nat Nanotechnol*, 2011, **6**, 517-523.
10. Y. Hu, P. Geissinger and J. C. Woehl, *Journal of Luminescence*, 2011, **131**, 477-481.
11. J. J. Leonard, T. Yonetani and J. B. Callis, *Biochemistry*, 1974, **13**, 1460-1464.
12. M. P. Bruchez, *Current opinion in chemical biology*, 2015, **27**, 18-23.
13. J. L. Anderson, C. T. Armstrong, G. Kodali, B. R. Lichtenstein, D. W. Watkins, J. A. Mancini, A. L. Boyle, T. A. Farid, M. P. Crump, C. C. Moser and P. L. Dutton, *Chem Sci*, 2014, **5**, 507-514.
14. J. D. Brodin, X. I. Ambroggio, C. Tang, K. N. Parent, T. S. Baker and F. A. Tezcan, *Nature chemistry*, 2012, **4**, 375-382.
15. K. Oohora and T. Hayashi, *Current opinion in chemical biology*, 2014, **19**, 154-161.
16. K. Oohora, T. Mashima, K. Ohkubo, S. Fukuzumi and T. Hayashi, *Chemical communications*, 2015, **51**, 11138-11140.
17. P. A. Sontz, W. J. Song and F. A. Tezcan, *Current opinion in chemical biology*, 2014, **19**, 42-49.
18. H. Anni, J. M. Vanderkooi and L. Mayne, *Biochemistry*, 1995, **34**, 5744-5753.
19. J. M. Vanderkooi, F. Adar and M. Erecinska, *European Journal of Biochemistry*, 1976, **64**, 381-387.
20. E. A. Della Pia, Q. Chi, M. Elliott, J. E. Macdonald, J. Ulstrup and D. D. Jones, *Chemical communications*, 2012, **48**, 10624-10626.
21. M. W. Schmidt, K. K. Baldridge, J. A. Boatz, S. T. Elbert, M. S. Gordon, J. H. Jensen, S. Koseki, N. Matsunaga, K. A. Nguyen, S. Su, T. L. Windus, M. Dupuis and J. A.

Montgomery, *Journal of Computational Chemistry*, 1993, **14**, 1347-1363.
22. F. Arnesano, L. Banci, I. Bertini, J. Faraone-Mennella, A. Rosato, P. D. Barker and A. R. Fersht, *Biochemistry*, 1999, **38**, 8657-8670.
23. Y. Feng, S. G. Sligar and A. J. Wand, *Nat Struct Biol*, 1994, **1**, 30-35.
24. F. Lederer, A. Glatigny, P. H. Bethge, H. D. Bellamy and F. S. Matthew, *Journal of molecular biology*, 1981, **148**, 427-448.
25. E. A. Della Pia, Q. Chi, D. D. Jones, J. E. Macdonald, J. Ulstrup and M. Elliott, *Nano letters*, 2011, **11**, 176-182.
26. E. A. Della Pia, Q. Chi, J. E. Macdonald, J. Ulstrup, D. D. Jones and M. Elliott, *Nanoscale*, 2012, **4**, 7106-7113.
27. P. Wittung-Stafshede, J. C. Lee, J. R. Winkler and H. B. Gray, *Proceedings of the National Academy of Sciences of the United States of America*, 1999, **96**, 6587-6590.
28. P. Zuo, T. Albrecht, P. D. Barker, D. H. Murgida and P. Hildebrandt, *Physical chemistry chemical physics : PCCP*, 2009, **11**, 7430-7436.
29. J. D. Brodin, A. Medina-Morales, T. Ni, E. N. Salgado, X. I. Ambroggio and F. A. Tezcan, *Journal of the American Chemical Society*, 2010, **132**, 8610-8617.
30. E. A. Della Pia, J. E. Macdonald, M. Elliott and D. D. Jones, *Small*, 2012, **8**, 2341-2344.
31. D. D. Jones and P. D. Barker, *Chembiochem*, 2004, **5**, 964-971.
32. S. Takeda, N. Kamiya and T. Nagamune, *Biotechnol Lett*, 2004, **26**, 121-125.
33. Y. Tokita, S. Yamada, W. Luo, Y. Goto, N. Bouley-Ford, H. Nakajima and Y. Watanabe, *Angewandte Chemie*, 2011, **50**, 11663-11666.
34. J. A. Arpino, H. Czapinska, A. Piasecka, W. R. Edwards, P. Barker, M. J. Gajda, M. Bochtler and D. D. Jones, *Journal of the American Chemical Society*, 2012, **134**, 13632-13640.
35. R. J. Radford and F. A. Tezcan, *Journal of the American Chemical Society*, 2009, **131**, 9136-9137.
36. A. Onoda, Y. Kakikura, T. Uematsu, S. Kuwabata and T. Hayashi, *Angewandte Chemie*, 2012, **51**, 2628-2631.
37. W. R. Scheidt, J. U. Mondal, C. W. Eigenbrot, A. Adler, L. J. Radonovich and J. L. Hoard, *Inorganic Chemistry*, 1986, **25**, 795-799.
38. F. A. Tezcan, B. R. Crane, J. R. Winkler and H. B. Gray, *Proceedings of the National Academy of Sciences of the United States of America*, 2001, **98**, 5002-5006.
39. N. D'Amelio, A. M. Bonvin, M. Czisch, P. Barker and R. Kaptein, *Biochemistry*, 2002, **41**, 5505-5514.
40. G. M. Morris, R. Huey, W. Lindstrom, M. F. Sanner, R. K. Belew, D. S. Goodsell and A. J. Olson, *J Comput Chem*, 2009, **30**, 2785-2791.
41. J. Meiler and D. Baker, *Proteins*, 2006, **65**, 538-548.
42. N. C. Shaner, P. A. Steinbach and R. Y. Tsien, *Nat Methods*, 2005, **2**, 905-909.
43. R. Y. Tsien, *Annual review of biochemistry*, 1998, **67**, 509-544.
44. J. Zhang, R. E. Campbell, A. Y. Ting and R. Y. Tsien, *Nat Rev Mol Cell Biol*, 2002, **3**, 906-918.
45. A. P. Demchenko, *Luminescence*, 2002, **17**, 19-42.
46. D. A. M. Catici, H. E. Amos, Y. Yang, J. M. H. van den Elsen and C. D. Pudney, *FEBS J*, 2016, **In Press**.
47. T. Komatsu, R. M. Wang, P. A. Zunszain, S. Curry and E. Tsuchida, *Journal of the American Chemical Society*, 2006, **128**, 16297-16301.